0026-895X/04/6506-1336–1343$20.00
MOLECULAR PHARMACOLOGY
Copyright © 2004 The American Society for Pharmacology and Experimental Therapeutics
Mol Pharmacol 65:1336–1343, 2004

Vol. 65, No. 6
3029/1151019
Printed in U.S.A.

Discovery of Novel Selective Inhibitors of Human Intestinal Carboxylesterase for the Amelioration of Irinotecan-Induced Diarrhea: Synthesis, Quantitative Structure-Activity Relationship Analysis, and Biological Activity

Randy M. Wadkins, Janice L Hyatt, Kyoung Jin P. Yoon, Christopher L. Morton, Richard E. Lee, Komath Damodaran, Paul Beroza, Mary K. Danks, and Philip M. Potter

Department of Chemistry and Biochemistry, University of Mississippi, University, Mississippi (R.M.W.); Department of Molecular Pharmacology, St. Jude Children's Research Hospital, 332 N. Lauderdale, Memphis, Tennessee (J.L.H., K.J.P.Y., C.L.M., M.K.D., P.M.P.); Department of Pharmaceutical Sciences, University of Tennessee Health Science Center, Memphis, Tennessee (R.E.L.); and Computational Sciences, Telik Inc., Palo Alto, California (K.D., P.B.)

Received October 13, 2003; accepted February 19, 2004

This article is available online at http://molpharm.aspetjournals.org

ABSTRACT

The dose-limiting toxicity of the highly effective anticancer agent 7-ethyl-10-[4-(1-piperidino)-1-piperidino]carbonyloxycamptothecin (irinotecan; CPT-11) is delayed diarrhea. This is thought to be caused by either bacteria-mediated hydrolysis of the glucuronide conjugate of the active metabolite 7-ethyl-10-hydroxycamptothecin (SN-38) or direct conversion of CPT-11 to SN-38 by carboxylesterases (CE) in the small intestine. After drug administration, a very high level of CPT-11 is present in the bile; this is deposited into the duodenum, the region of the gut with the highest levels of CE activity. Hence, it is likely that direct conversion of the drug to SN-38 is partially responsible for the diarrhea associated with this agent. In an attempt to ameliorate this toxicity, we have applied Target-Related Affinity Profiling to identify novel CE inhibitors that are selective inhibitors of the human intestinal enzyme (hiCE). Seven inhibitors, all sulfonamide derivatives, demonstrated greater than 200-fold selectivity for hiCE compared with the human liver CE hCE1, and none was an inhibitor of human acetylcholinesterase or butyrylcholinesterase. Quantitative structure-activity relationship (QSAR) analysis demonstrated excellent correlations with the predicted versus experimental K_i values ($r^2 = 0.944$) for hiCE. Additionally, design and synthesis of a tetrafluorine-substituted sulfonamide analog, which QSAR indicated would demonstrate improved inhibition of hiCE, validated the computer predictive analyses. These and other phenyl-substituted sulfonamides compounds are regarded as lead compounds for the development of effective, selective CE inhibitors for clinical applications.

7-Ethyl-10-[4-(1-piperidino)-1-piperidino]carbonyloxycamptothecin) (irinotecan, CPT-11) is a camptothecin-derived prodrug that is activated by esterases to yield 7-ethyl-10-hydroxycamptothecin (SN-38), a potent topoisomerase I inhibitor (Tsuruo et al., 1988; Satoh et al., 1994; Tanizawa et al., 1994; Sawada et al., 1996). This drug has demonstrated remarkable antitumor activity in human tumor xenograft models and consequently has been developed for clinical studies in a variety of tumor histotypes (Houghton et al., 1995, 1996; Thompson et al., 1997a,b; Furman et al., 1999). Currently, CPT-11 is approved for use in colorectal cancer, but is in phase I, II, and III trials for treatment of many solid tumors in both adults and children (Furman et al., 1999).

In humans, CPT-11 activation is primarily mediated by carboxylesterases (CE) present in the liver and intestine. Drug hydrolysis is required for antitumor efficacy, and because the parent molecule and metabolites are cleared from the circulation via the bile, very high concentrations of CPT-11 and SN-38 can be detected in this fluid (Morton et al., 2002). Because the bile duct opens into the duodenum, the region of the gut with the highest level of CE activity (Morton et al., 2002), direct activation of CPT-11 by CEs would result

This work was supported in part by National Institutes of Health Cancer Center Core grant P30-CA21765 and by the American Lebanese Syrian Associated Charities.

ABBREVIATIONS: CPT-11, irinotecan, 7-ethyl-10-[4-(1-piperidino)-1-piperidino]carbonyloxycamptothecin; SN-38, 7-ethyl-10-hydroxycamptothecin; CE, carboxylesterase; hiCE, human intestinal carboxylesterase; AcChE, acetylcholinesterase; BuChE, butyrylcholinesterase; TRAP, Target Related Affinity Profiling; BNPP, bis(4-nitrophenyl) phosphate; rCE, rabbit liver carboxylesterase; hCE1, human carboxylesterase 1; *o*-NP, *o*-nitrophenol; *o*-NPA, *o*-nitrophenyl acetate; hAcChE, human acetylcholinesterase; hBuChE, human butyrylcholinesterase; DMSO, dimethyl sulfoxide; 3D, three dimensional; QSAR, quantitative structure-activity relationship; HPLC, high performance liquid chromatography.

in increased levels of SN-38 and hence enhanced toxicity to the small intestine. This would account for the delayed diarrhea caused by mucosal damage that is observed in patients undergoing therapy with this drug.

To alleviate this dose-limiting and potentially life threatening toxicity, we hypothesized that the development of specific human intestinal esterase inhibitors that would prevent the conversion of CPT-11 to SN-38 in the gut might ameliorate these side effects. Recently, we identified the enzyme responsible for CPT-11 activation in the small intestine, human intestinal CE (hiCE), and demonstrated that expression of this protein in mammalian cells sensitized them to the drug (Khanna et al., 2000). This enzyme is highly homologous to the human liver CE 2, and both proteins are probably the products of the same gene (Potter and Danks, 2000). Therefore, in the current study, we have attempted to identify selective inhibitors of hiCE that would not inhibit other human CEs, acetylcholinesterases (AcChE), or butyrylcholinesterase (BuChE). Using a directed screening procedure based upon Telik's Target-Related Affinity Profiling (TRAP) technology (Kauvar et al., 1995; Dixon and Villar, 1998; Beroza et al., 2002) with purified CEs, we have identified a novel class of enzyme inhibitors that demonstrates selectivity and specificity for hiCE.

TABLE 1
Name and chemical structures of the hiCE-specific sulfonamide derived carboxylesterase inhibitors.

ID	Name	Structure
1	4-Chloro-*N*-(4-{[(4-chlorophenyl) sulfonyl]amino}phenyl) benzenesulfonamide	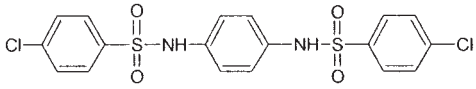
2	*N*-{2,3,5,6-Tetrachloro-4-[(phenylsulfonyl) amino]phenyl} benzenesulfonamide	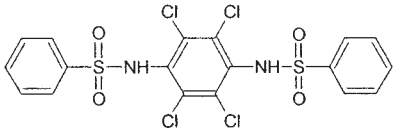
3	4,6-Dimethyl-*N*,*N*′-diphenylbenzene-1,3-disulfonamide	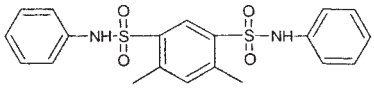
4	4-Chloro-*N*-(4-{[(4-chlorophenyl)sulfonyl] amino}-1-naphthyl) benzenesulfonamide	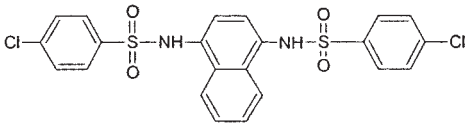
5	4-Bromo-*N*-(4-phenoxyphenyl) benzenesulfonamide	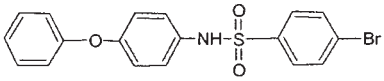
6	*N*-{2-Methyl-4-[(phenylsulfonyl)amino]phenyl} benzenesulfonamide	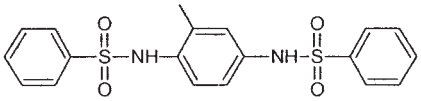
7	*N*-[4-({4-[(Methylsulfonyl)amino]phenyl}dithio) phenyl] methanesulfonamide	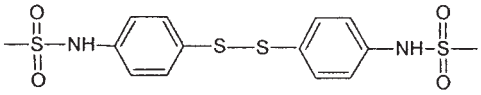
8	*N*-{4-[(Phenylsulfonyl)aminophenyl} benzenesulfonamide	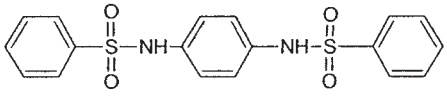
9	4-Chloro-*N*-(4-ethoxyphenyl) benzenesulfonamide	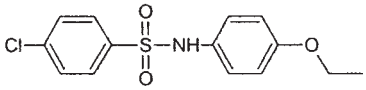
10	4-Chloro-*N*-(4-{[(4-chlorophenyl)sulfonyl]amino} 2,3,5,6-tetrafluorophenyl) benzenesulfonamide	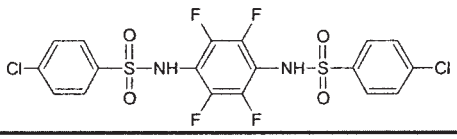

Materials and Methods

Drugs and Inhibitors. CPT-11 was kindly provided by Dr. J.P. McGovren (Pharmacia Upjohn, Piscataway, NJ). Bis(4-nitrophenyl) phosphate (BNPP) was obtained from Sigma Biochemicals (St. Louis, MO).

Purified Enzymes. Pure rabbit liver CE (rCE) and hCE1 were prepared from baculovirus-infected cell culture media as described previously (Morton and Potter, 2000). hiCE was prepared in a similar fashion, although the samples were only ~60% pure. Because serum-free media harvested from insect cells is essentially devoid of CE activity (Morton and Potter, 2000), the only enzyme present in the preparation was recombinant hiCE. The cDNA sequences encoding the above proteins have the following GenBank accession numbers; rCE, AF036930 (Potter et al., 1998); hCE1, M73499 (Munger et al., 1991); and hiCE, Y09616 (Schwer et al., 1997). All enzymes were characterized using *o*-nitrophenyl acetate (*o*-NPA; Sigma Chemicals, St. Louis, MO) as a substrate (Beaufay et al., 1974; Potter et al., 1998), and preparations were stored at 4°C in 50 mM HEPES, pH 7.4. Human AcChE (hAcChE) and BuChE (hBuChE) were purchased from Sigma and stored at 4°C.

Library of Inhibitors. The compounds for screening were selected from Telik's library of small molecules using the TRAP methodology (Dixon and Villar, 1998). TRAP characterizes a molecule by its binding affinities to a panel of proteins (i.e., its "affinity fingerprint"). The screening process is iterative, with ~70 compounds being tested at each iteration. The first set of compounds is chosen because their fingerprints represent the diversity of fingerprints in the entire compound collection. Subsequent iterations are based on computational analysis of the fingerprints of the compounds that were screened in previous rounds of analysis. This process allows identification of active compounds of multiple chemotypes by assaying as few as 200 compounds (Dixon and Villar, 1998; Beroza et al., 2002).

Carboxylesterase Assays. CE activity was determined as described previously (Beaufay et al., 1974; Potter et al., 1998). One unit is the amount of enzyme that converts 1 μmol of *o*-NPA to *o*-nitrophenol per minute.

Carboxylesterase Enzyme Inhibition Assays. All inhibitors were dissolved in DMSO, typically at 10 mM, before analysis. For screening enzyme inhibitors, 100 μl of HEPES, pH 7.4, containing 6 mM *o*-NPA and 200 μM test compound were added to each well of a 96-well plate. The reaction was initiated by adding 100 μl of the appropriate CE containing 20 to 30 units of enzyme, and the absorbance was monitored at 15-s intervals for 5 min. All compounds were assayed in duplicate, and all plates included positive (50 μM BNPP) and negative (no enzyme, DMSO alone) controls. DMSO concentrations never exceeded 2% and routinely were 1% or less. Compounds that demonstrated greater than 50% inhibition of CE activity were further characterized by determining their K_i values with the appropriate enzyme.

Determination of K_i Values. K_i values for the inhibitors were determined with either 3 mM *o*-NPA or 100 μM CPT-11 as substrates. At least eight inhibitor concentrations were used for the analyses, and the data were fitted to one of six equations describing competitive, partially competitive, noncompetitive, partially noncompetitive, mixed, or uncompetitive inhibition (Webb, 1963). These equations are described below:

$$\text{Competitive inhibition:} \quad i = \frac{[I]}{[I] + K_i\left(1 + \frac{[s]}{[K_s]}\right)} \tag{1}$$

Assume $\alpha = \infty$

$$\text{Partially competitive:} \quad i = \frac{[I](\alpha - 1)}{[I]\left(\alpha + \frac{[s]}{[K_s]}\right) + \alpha K_i\left(1 + \frac{[s]}{[K_s]}\right)} \tag{2}$$

Assume $1 < \alpha < \infty$; $\beta = 1$

$$\text{Noncompetitive:} \quad i = \frac{[I]}{[I] + K_i} \tag{3}$$

Assume $\alpha = 1$; $\beta = 0$

$$\text{Partially noncompetitive:} \quad i = (1 - \beta)\frac{[I]}{[I] + K_i} \tag{4}$$

Assume $\alpha = 1$; $0 < \beta < 1$

$$\text{Mixed:} \quad i = \frac{[I]}{[I] + K_i\left\{\frac{(\alpha[s] + \alpha K_s)}{([s] + \alpha K_s)}\right\}} \tag{5}$$

Assume $1 < \alpha < \infty$; $\beta = 0$

$$\text{Uncompetitive:} \quad i = \frac{[I]}{[I] + K_i'\left(1 + \frac{K_s}{[s]}\right)} \tag{6}$$

Assume $\alpha < 1$; $\beta < 1$.

In each case, i is fractional inhibition, $[s]$ is substrate concentration, $[I]$ is inhibitor concentration, α is change in affinity of substrate for enzyme, β is change in the rate of enzyme substrate complex decomposition, and K_s is the dissociation constant for the enzyme substrate complex.

After fitting the data to these equations using Prism (GraphPad Software, San Diego, CA), r^2 values were determined for each set of results. Using both the r^2 value and the statistical analysis of these curve fits, assignment of the mode of enzyme inhibition was performed.

Acetylcholinesterase Enzyme Assays. AcChE assays were performed using a spectrophotometric multiwell plate assay (Doctor et

TABLE 2

Analysis of the mode of hiCE inhibition, and K_i values when using *o*-NPA as a substrate, for the sulfonamides. K_i values were determined from the equation yielding the greatest r^2 value (indicated in bold).

Compound	r^2 for Data Values Using Indicated Mode of Enzyme Inhibition						$K_i \pm$ S.E.
	Competitive	Partially Competitive	Noncompetitive	Partially Noncompetitive	Mixed	Uncompetitive	
							nM
1	0.991	**0.997**	0.643	0.083	0.991	0.991	53.3 ± 5.5
2	0.972	**0.996**	0.972	0.120	0.972	0.972	451 ± 39
3	0.967	**0.988**	0.967	0.050	0.967	0.967	218 ± 45
4	0.754	**0.992**	0.754	0.151	0.754	0.754	194 ± 23
5	0.606	**0.980**	0.606	0.150	0.606	0.606	165 ± 33
6	0.964	**0.984**	0.250	0.071	0.964	0.964	365 ± 87
7	0.857	**0.945**	0.857	0.064	0	0.857	767 ± 285
8	0.971	**0.991**	0.971	0.080	0.978	0.971	1060 ± 133
9	0.959	**0.987**	0.959	0.104	0.959	0.959	1310 ± 176

al., 1987) using acetylthiocholine as a substrate (Ellman et al., 1961). Compounds were assayed at a final concentration of 100 μM with the DMSO concentration never exceeding 2%.

Butyrylcholinesterase Enzyme Assays. BuChE assays were performed as described above for AcChE, except that butyrylthiocholine was used as a substrate.

Determination of Irreversible Inhibition. To assess whether the inhibitors produced irreversible inhibition of hiCE, compounds were added to enzyme and incubated for 1 h on ice. Samples were then diluted in HEPES, pH 7.4, and CE activity was determined using a spectrophotometric assay with *o*-NPA as a substrate (Beaufay et al., 1974; Potter et al., 1998). Final concentrations of inhibitor in the assay reactions did not exceed 40 nM. CE activity was calculated as determined above, and results were expressed relative to control enzyme samples that were incubated with DMSO alone. The irreversible inhibitor BNPP was used as a positive control for these reactions.

Quantitation of CPT-11 and SN-38 by HPLC. CPT-11 and SN-38 concentrations were determined using an HPLC-based assay with a fluorescent detector as described previously(Guichard et al., 1998; Danks et al., 1999).

QSAR Analysis. 3D-QSAR analyses were performed using Quasar 4.0 (Vedani and Dobler, 2002a,b) running on a Macintosh G4. Structures for each analog were initially constructed with Chem3D for Macintosh. Partial atomic charges from the bond charge correction method (Jakalian et al., 2002) and AMBER atom types were assigned using the *antechamber* module of AMBER7 (University of California, San Francisco, CA). To select optimal conformers for 3D-QSAR, a short molecular dynamics run (250 ps) was performed at 500 K using the *sander* module of AMBER7. Snapshots were captured at 25-ps intervals, and the sulfonamide structures minimized with respect to energy with the AMBER95 force field.

Synthesis of 4-Chloro-*N*-(4-{[(4-chlorophenyl)sulfonyl] amino}-2,3,5,6-tetrafluorophenyl) benzenesulfonamide (10). To a stirred solution of 2,3,5,6-tetrafluorobenzene-1,4-diamine (0.2 g, 1.1 mmol) in anhydrous dichloromethane, 4-chlorobenzyl sulfonylchloride (1.4 g, 6.6 mmol), 4-(dimethylamino)-pyridine (0.13 g, 1.1 mmol), and pyridine (1.1g, 13.9 mmol) were added under an atmosphere of argon. The reaction mixture was stirred for 12 h at room temperature, and thin-layer chromatography was performed to confirm that the reaction had gone to completion. After extraction with dichloromethane (3 × 20 ml), the organic layer was washed with 0.5 N HCl, followed by saturated sodium bicarbonate. After drying over anhydrous sodium sulfate, the crude product was purified by column chromatography using petroleum ether/ethyl acetate (4:1; v:v) to give an off-white solid (0.1 g). Melting point, 231 to 233°C; anal., ($C_{18}H_{10}Cl_2F_4N_2O_4S_2$); calc., (%) C 40.84, H 1.90, N 5.29; found, (%) C 41.03, H 1.92, N 5.23; ^{1}H NMR (300 MHz, $CDCl_3$) δ 4.4 (s, 2H, N*H* x 2), 7.56 (d, 4H, J = 13.8 MHz, Ar-*H*), 7.95 (d, 4H, J = 13.8 MHz, Ar-*H*); ^{13}C NMR (75.5 MHz, $CDCl_3$) δ 147.2, 139.8, 140.8 126.8, 133.9, 129.6, 128.9; mass spectroscopy (electrospray ionization) *m/z* 527 (M-1).

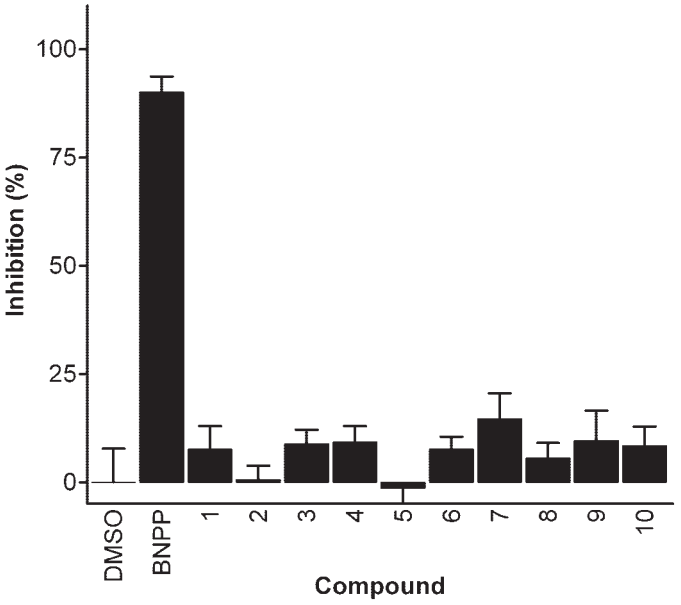

Fig. 1. CE activity in enzyme preparations after preincubation with different sulfonamide inhibitors. Enzyme activity was determined after incubation for 1 h with concentrations of 10 μM inhibitor. Irreversible inhibition was only observed with the control compound BNPP.

Results

Identification of Selective hiCE Inhibitors. Selective hiCE inhibitors were identified from four iterations of screening, a total of 235 compounds. Each compound was assayed against hiCE, hCE1, and rCE. After each round of screening, compounds were selected based upon their ability to selectively inhibit hiCE compared with hCE1. After four iterations of screening, nine novel sulfonamide analogs were identified that demonstrated hiCE-specific enzyme inhibition; 6 of these demonstrated at least 250-fold selectivity compared with hCE1 by examination of the K_i values. The ID, chemical name, and structures of these compounds are shown in Table 1.

The K_i values were determined for several different enzymes, including two human CEs, hiCE and hCE1, rCE, hAcChE, and hBuChE. Because accurate calculation of the K_i value is dependent upon the mode of inhibition, we fitted the assay results to six different equations describing the various mechanisms of enzyme inhibition. Analysis of the curve fits for these data and subsequent statistical calculations demonstrated that partially competitive inhibition (eq. 2) was the

TABLE 3

K_i values for the sulfonamide analogs with hiCE, hCE1, hAcChE, hBuChE, and rCE

o-NPA was used as a substrate with the CEs, and acetylthiocholine and butyrylthiocholine were used for hAcChE and hBuChE, respectively.

ID	hiCE K_i ± SE	hCE1 K_i ± SE	hAcChE K_i	hBuChE K_i	rCE K_i ± SE	Ratio hCE1 K_i/hiCE K_i
			nM			
1	53.3 ± 5.5	13,700 ± 4870	>100,000	>100,000	1200 ± 230	>250
2	451 ± 39	>100,000	>100,000	>100,000	>100,000	>220
3	218 ± 45	>100,000	>100,000	>100,000	>100,000	>450
4	194 ± 23	>100,000	>100,000	>100,000	>100,000	>510
5	165 ± 33	>100,000	>100,000	>100,000	319 ± 37	>250
6	365 ± 87	>100,000	>100,000	>100,000	3230 ± 439	>600
7	767 ± 285	>100,000	>100,000	>100,000	739 ± 384	>130
8	1060 ± 133	>100,000	>100,000	>100,000	1550 ± 350	>90
9	1310 ± 176	>100,000	>100,000	>100,000	2000 ± 755	>75

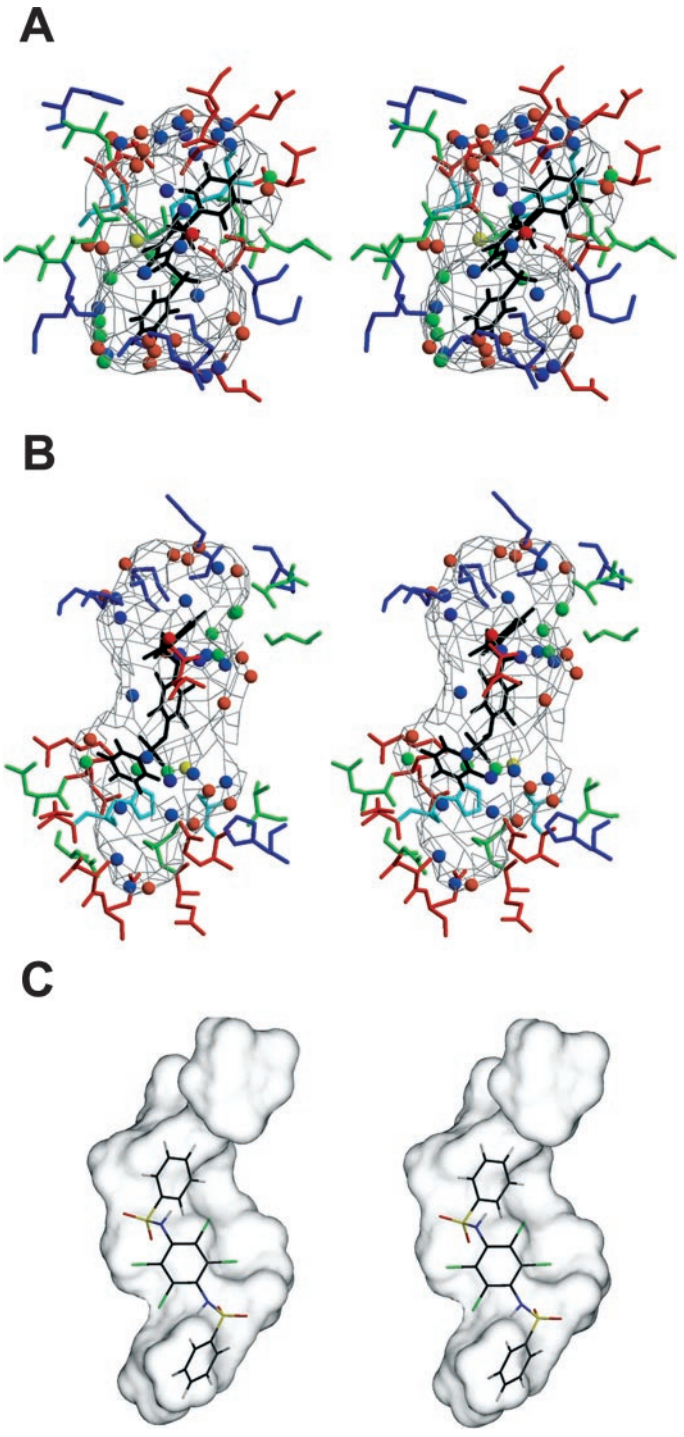

Fig. 2. The pseudo-receptor model of the sulfonamide binding site overlaid onto the structure of human intestinal CE. A and B, the pseudo-receptor sites (spheres) are colored according to charge or hydrogen-bonding potential. The spheres represent sites that are fully positively charged (blue), partially positively charged (light blue), hydrogen bond-donating (green), hydrogen bond-accepting (yellow), partially negatively charged (red-orange), and fully negatively charged (red). The gray bonded area represents sites that are hydrophobic only, and the structure of the sulfonamide **2** is shown in black. The residues lining the hiCE active site gorge are correspondingly colored: His, Arg, and Lys are blue; Ser, Thr, Asn, and Gln are green; and Asp and Glu are red. The active site Ser and His residues are shown in cyan. The view in A is looking directly into the gorge; in B, the structure is rotated 90° to provide a side view. The pseudo-receptor model reproduces most of the features of the active site gorge. C, the effectiveness of the sulfonamides in inhibiting hiCE is probably caused by their ability to match the shape of the active site gorge of the enzyme. The active site gorge is shown as a molecular surface (gorge opening at the top and catalytic residues at the bottom, with the sulfonamide **2** positioned within its interior. The almost identical molecular shape of the inhibitor and gorge probably contributes to the activity of this class of molecules. These images were produced with Molscript (Kraulis, 1991), Raster3D (Merritt and Bacon, 1997), and PASS (Brady and Stouten, 2000).

most appropriate model describing the interaction of the sulfonamides with hiCE (Table 2). As can be seen, r^2 values of 0.94 or above were generated for all compounds using this equation, and the calculated K_i values ranged from 53.3 to 1310 nM.

As indicated in Table 3, a 2-log range for the K_i values for hiCE was obtained. The majority of the compounds were bis-benzene sulfonamides, with the most potent compound (**1**: 4-chloro-*N*-(4-{[(4-chlorophenyl)sulfonyl]amino}phenyl) benzenesulfonamide) containing *p*-chloro-substituted benzene rings at either end of the molecule. This same compound demonstrated inhibition of hCE1 catalysis at concentrations below 100 μM; however, the K_i for **1** with hCE1 was at least 250-fold greater than that for hiCE (13,700 nM). More importantly, none of the compounds demonstrated any inhibition of hAcChE, or hBuChE, at concentrations up to 100 μM.

As indicated in Table 3, there was some overlap in the inhibition pattern for rCE. Because both hiCE and rCE can efficiently metabolize CPT-11, we expected some of the sulfonamide derivatives to inhibit both enzymes. However, even within this small series of compounds, apparent selectivity can be observed. For example, analogs **2**, **3**, and **4** were selective for hiCE, demonstrating greater than 220-fold selectivity compared with all other enzymes tested. In contrast, compounds **5** and **7** were effective inhibitors of both hiCE and rCE.

Determination of Reversibility of Enzyme Inhibition. To determine whether any of the inhibitors resulted in irreversible inhibition of hiCE, we preincubated enzyme preparations with the inhibitors at a concentration of 10 μM for 1 h, before CE activity assays. Because the enzyme and inhibitor were diluted at least 250-fold in the CE assay, loss of activity can only occur from direct inactivation of the protein by the sulfonamide analog during the preincubation period. None of the inhibitors resulted in permanent inhibition of the enzyme (Fig. 1), whereas 10 μM BNPP resulted in greater than 90% inhibition of hiCE. These results suggest that the sulfonamide analogs inhibited in a reversible fashion.

Inhibition of CPT-11 Metabolism of the Sulfonamide Analogs. Because the sulfonamide analogs are partially competitive inhibitors of hiCE, their K_i values will be dependent upon the substrates used in the kinetics analyses (see eq. 2). Therefore, to assess the ability of these compounds to inhibit hiCE-mediated activation of CPT-11, we determined the K_i values using the drug as a substrate. CPT-11 concentration was fixed at 100 μM, and inhibitor concentrations varied from 1 nM to 100 μM. After incubation for 10 min at 37°C, the levels of SN-38 in the reactions were determined by HPLC. Table 4 indicates that the K_i values for the inhibition of metabolism of CPT-11 are similar to those for the inhibition of *o*-NPA. However, several analogs did not inhibit drug metabolism. Because the sulfonamides are partially competitive inhibitors and the K_i is dependent upon the ratio of substrate concentration and K_m ([s]/K_m), it is likely that

these discrepancies are a result of the differences in the K_m values for the substrates. The K_m values for hiCE with CPT-11 and *o*-NPA are significantly different at 3.2 and 355 μM, respectively. Overall, these results suggest that although the sulfonamide analogs are potent CE inhibitors, it is apparent that their potency is substrate-dependent.

3D-QSAR Analysis of the Sulfonamide Analogs. Because we expected that the sulfonamides must fit into the active site gorge of the carboxylesterase for inhibition, and given the steric constraints on the diameter of this gorge, for 3D-QSAR we selected the most extended sulfonamide conformer from the pool of 10 conformers generated from the molecular dynamics simulation. These were aligned around the sulfonamido group of each inhibitor and model that predicted the activity of the inhibitors was then constructed. The pseudo-receptor model that best reproduced the sulfonamide K_i values is shown in Fig. 2. The properties of the pseudo-receptor are shown as color-coded spheres surrounding the sulfonamide compound **2**. The residues in the active site gorge are taken from our homology model of hiCE (Wadkins et al., 2001) and are matched in color-coding to the pseudo-receptor model. Note that the pseudo-receptor model reproduces the distribution of residue types very well, including the charge asymmetry within the gorge. The cationic His, Lys, and Arg residues (red) are located at the opening of the gorge and are clustered on one side of the opening. The anionic Asp and Glu residues (blue) are at the bottom of the gorge, and are clustered on the side of the gorge opposite that where the cationic residues are located. The gorge is lined with hydrophobic residues, which coincide with the predicted hydrophobic surface (gray lines) in the pseudoreceptor model. In summary, the 3D-QSAR captures the essential features of the hiCE active site gorge and can be used to predict activities of novel sulfonamides as hiCE inhibitors. Based on this information, we predicted that halogen substitution of the benzene rings would increase the potency of the inhibitors; hence, we synthesized a fluoro analog to test the validity of the QSAR approach.

Synthesis of Compound 10. Validation of QSAR Analysis. QSAR analysis indicated that compound **10** would be a very good inhibitor of hiCE, with a predicted K_i of ~390 nM when using *o*-NPA as a substrate. To assess the validity of this model, we synthesized compound **10** (Table 1) by condensation of 2,3,5,6-tetrafluorobenzene-1,4-diamine with *p*-chlorobenzenesulfonyl chloride. The ability of **10** to inhibit hiCE, hCE1, rCE, hAcChE, and hBuChE was then assessed using *o*-NPA for the CEs, acetylthiocholine for hAcChE, or butyrylthiocholine for hBuChE as substrates.

As indicated in Table 5, sulfonamide **10** was a very good inhibitor of hiCE, with a K_i value of 41.5 nM. This compound did not inhibit hCE1, hAcChE, or hBuChE, consistent with results seen with the other sulfonamide analogs. In addition, compound **10** acted in a partially competitive fashion, similar to that observed with sulfonamides **1** to **9**. Inhibition was observed when using rCE as an enzyme; as with the other sulfonamide-analogs, however, the K_i value (522 nM) was greater than that observed with hiCE. The K_i value predicted from the QSAR analyses for compound **10** with hiCE (393 nM) was near the observed value (41.5 nM), demonstrating both the validity of the technique and the potential use of the data to design inhibitors with greater specificity. It is noteworthy that sulfonamide **10** had the lowest K_i for the inhibition of CPT-11 metabolism by hiCE (110 nM; Table 5), for all of the compounds analyzed.

TABLE 4

K_i values for the sulfonamide analogs with hiCE using CPT-11 as a substrate.

ID	hiCE K_i ± SE
	nM
1	141 ± 64
2	>100,000
3	>100,000
4	>100,000
5	>100,000
6	238 ± 29
7	>100
8	892 ± 67
9	3220 ± 950

TABLE 5

K_i values for hiCE, hCE1, rCE, and hAcChE with compound **10** using either *o*-NPA, CPT-11, or acetylthiocholine as substrates

All values are nanomolar except for the ratio. Experimental values are presented ± S.E.

Experimental hiCE K_i (*o*-NPA)	41.5 ± 6.5
Predicted hiCE K_i (*o*-NPA)	393
hiCE K_i (CPT-11)	110 ± 23
hCE1 K_i (*o*-NPA)	>100,000
hAcChE K_i (acetylthiocholine)	>100,000
rCE K_i (*o*-NPA)	522 ± 144
Ratio hCE1 K_i/hiCE K_i (*o*-NPA)	>2400

Discussion

We have identified a novel class of CE inhibitors based upon the sulfonamide chemotype. These compounds are selective for hiCE, demonstrating no inhibition of a human liver CE, hCE1, hAcChE, or hBuChE. In addition, these sulfonamides are very potent inhibitors, with K_i values in the low nanomolar range. The analogs were identified through application of Telik's TRAP technology after screening of a diverse chemical library. One class of molecules identified in the TRAP screen typically contained two sulfonamide moieties, usually present as a symmetrical molecule. In addition, the majority of these analogs contained phenyl rings both in the central and terminal domains of the structures.

Halogen substitution of benzene rings tended to increase the potency of the inhibitors (e.g., **1** > **2** > **8**), suggesting that withdrawal of the π electrons from the rings may influence binding of the sulfonamide within the CE active site. We therefore hypothesized that sulfonamide **10** might be a better inhibitor of hiCE. Subsequent studies confirmed this prediction; compound **10** had a K_i for hiCE with *o*-NPA of 41.5 nM. These results suggest that chemical substitutions that alter the localization of electrons within the sulfonamide moiety significantly affect the level of enzyme inhibition. Furthermore, we propose that the overall molecular structure of the sulfonamides contributes to their activity. As shown in Fig. 2C, the compounds adopt a conformation that is complementary to the computer-predicted model of the active site gorge of hiCE (shown as a surface representation). Hence, the combination of electronic and structural elements for this class of compounds allows for localization within, and interaction with, the residues that form the boundaries of the active site.

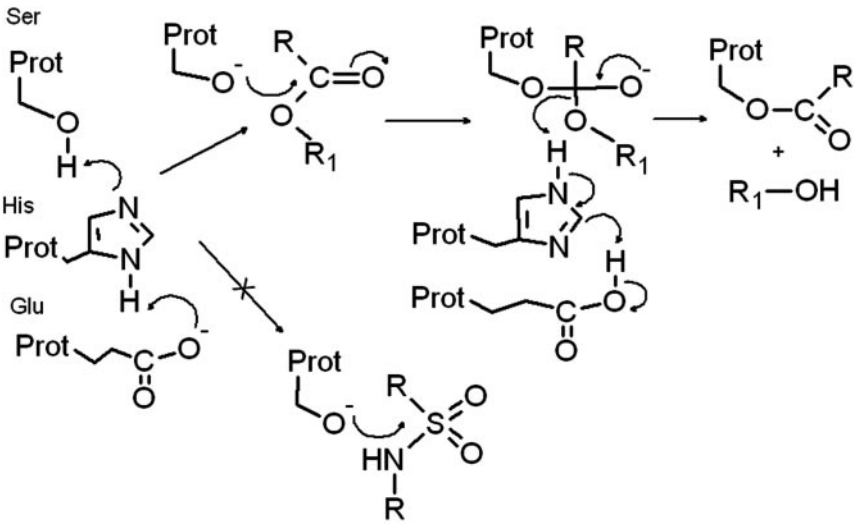

Fig. 3. Initial mechanism of catalysis by carboxylesterases. Generation of the serine nucleophile is accomplished by sequential transfer of the proton to the histidine and then glutamic acid. The resulting O^- can then attack the carbonyl carbon in the ester to yield a transient tetrahedral intermediate. This intermediate is trapped after reaction of CEs with organophosphates, such as sarin. Subsequent reformation of the carbonyl bond results in loss of the tetrahedral complex and liberation of the alcohol (R_1OH). As indicated, attack of the sulfur atom in the sulfonamide by the O^- nucleophile does not occur. More likely, the inhibitor forms hydrogen-bonds with protons within the active site and the sulfonyl oxygen atoms, essentially preventing access of the substrate to the catalytic amino acids. The curly arrows indicate the movement of a pair of electrons. The conserved active site residues for all CEs, Ser, His, Glu, and the protein backbone (Prot) are indicated.

The K_i values for the inhibition of CE-mediated metabolism of CPT-11 by the sulfonamides were significantly greater compared with those derived from using *o*-NPA as a substrate. This is partly because the K_m for hiCE for CPT-11 is approximately 100-fold lower than that for *o*-NPA (3.2 μversus 355 μM). Because these inhibitors are competitive, the efficacy of inhibition is dependent on the affinity of both the sulfonamide and the substrate for the enzyme. However, as indicated in Tables 4 and 5, several of the analogs were effective inhibitors of CPT-11 metabolism; the greatest inhibition was observed from compound **10**. Because this was proposed as an effective agent from the analysis the SAR studies, these results support the development of novel sulfonamide-based CE inhibitors using computational methods.

Esterase-mediated catalysis occurs in a four-stage reaction initiated by the nucleophilic attack of the carbonyl carbon by the deprotonated OH group in the serine amino acid at the active site (Fig. 3). This is followed by elimination of the alcohol and water, after attack by an HO^- moiety. Potentially, the sulfur atom present in the inhibitors could act as a site of initial attack by the O^- nucleophile, resulting in a square pyramidal intermediate. However, nucleophilic attack of the sulfur atom in sulfonamides requires very harsh chemical conditions; therefore, the formation of the covalently bound transient intermediate is not favored. Although this mechanism has been proposed for sulfonamide-based inhibitors of matrix metalloproteinases and thrombin, crystallographic and computer homology studies with these compounds in complex with the proteins indicate that this does not occur (Brandstetter et al., 1992; MacPherson et al., 1997; Kiyama et al., 1999; Whittaker et al., 1999). Rather, a network of hydrogen bonding between the sulfonyl oxygen atoms and protons exposed within the active site was observed. This stabilizes the sulfonamide-protein complex and presumably prevents access of the substrate to the catalytic amino acids. Thrombin has a catalytic triad of amino acids (Ser, His, and Asp rather than Glu) and a mechanism of substrate cleavage similar to observed in CEs. Hence, it is likely that the mechanism of inhibition of thrombin by sulfonamides would be comparable with inhibition of CEs by this class of compounds.

On the other hand, the sulfonamides may act as inhibitors by mimicking the CE transition state. The first stage in CE-mediated catalysis is the formation of a negatively charged tetrahedral intermediate involving nucleophilic attack by Ser toward the carbonyl carbon of the ester (see Fig. 3). As the sulfonamide chemotype in the compounds described in Table 1, would also adopt a tetrahedral and partially negatively charged conformation at physiological pH, this might act to inhibit catalysis by binding to the active site and blocking enzyme function. Inhibition by transition state analogs is a well validated drug design strategy that has led to the clinical development of protease and glycosidase inhibitors.

Because the sulfonamide-derived hiCE inhibitors contain multiple phenyl rings, they would prefer to localize within regions of the protein that are hydrophobic. Because the active sites of CEs are lined with aromatic amino acids, the gorge leading to the catalytic triad is very hydrophobic, thereby providing a suitable binding pocket for the sulfonamide analogs. Because compounds containing structurally similar functional groups (e.g., benzyl-substituted sulfoxides and sulfones) demonstrated no inhibition of CEs (data not shown), it is likely that resonance of the protons between the sulfur and nitrogen atoms is important for biological activity. Studies to determine the mechanism of inhibition by the sulfonamides using NMR and X-ray crystallography are currently underway.

Previously identified esterase inhibitors have included carbamates (physostigmine, pirimicarb), organophosphates (sarin, VX gas), acridines (e.g., tacrine, 9-amino-6-chloro-2-methoxyacridine), and piperidines (e.g., donepezil, CPT-11). None of these classes of compounds contains the sulfonamide function. Proteases, which demonstrate active site geometry and catalytic amino acid residues very similar to those of esterases, can be inhibited by sulfonyl chlorides and fluorides (e.g., phenylmethylsulfonyl fluoride), and these compounds have been used as protease inhibitors for many years. These agents are known to react directly with the serine at the active site, with the loss of the halogen, to yield a sulfonylated adduct and an inactive protein. Although, in theory, the sulfonylated enzyme could be reactivated, this requires harsh chemical conditions (pH 2.0, 40°C, 3 h) followed by neutralization and extensive dialysis. We propose that the sulfonamide-CE interaction occurs via a different mechanism, because our results indicate that the compounds iden-

tified in this report are reversible esterase inhibitors and do not form stable long-lived intermediates. More likely, they yield transient complexes stabilized by hydrogen bonding between the sulfonyl oxygen atoms and protons within the active site gorge (Kiyama et al., 1999). This mechanism would allow for the rapid reversal of the complexes to yield the free enzyme and inhibitor and would constitute a novel mechanism of CE inhibition by the sulfonamide analogs.

For clinical application, we predict that a poorly bioavailable compound would prove the most efficacious for reducing hiCE-mediated CPT-11 activation. The sulfonamide would be administered orally with the intention of maintaining high concentrations of inhibitor within the lumen of the gut. Systemic absorption of the compound would be low, so no change in the antitumor efficacy of CPT-11 would be encountered. However, inhibition of hiCE present within the gut epithelia would occur, eliminating in situ activation of drug and hence the delayed diarrhea associated with CPT-11 administration. We are currently assessing the efficacy of enzyme inhibition by the sulfonamides in animal models. In addition, we are further analyzing the mechanism of enzyme inhibition by conducting structural studies with selected sulfonamides in complex with hiCE.

Acknowledgments

We thank Dr. J. P. McGovren for the gift of CPT-11.

References

Beaufay H, Amar-Costesec A, Feytmans E, Thines-Sempoux D, Wibo M, Robbi M, and Berthet J (1974) Analytical study of microsomes and isolated subcellular membranes from rat liver. I. Biochemical methods. *J Cell Biol* **61:**188–200.

Beroza P, Villar HO, Wick MM, and Martin GR (2002) Chemoproteomics as a basis for post-genomic drug discovery. *Drug Discov Today* **7:**807–814.

Brady GP and Stouten PF (2000) Fast prediction and visualization of protein binding pockets with PASS. *J Comput-Aided Mol Des* **14:**383–401.

Brandstetter H, Turk D, Hoeffken HW, Grosse D, Sturzebecher J, Martin PD, Edwards BF, and Bode W (1992) Refined 2.3 A X-ray crystal structure of bovine thrombin complexes formed with the benzamidine and arginine-based thrombin inhibitors NAPAP, 4-TAPAP and MQPA. A starting point for improving antithrombotics. *J Mol Biol* **226:**1085–1099.

Danks MK, Morton CL, Krull EJ, Cheshire PJ, Richmond LB, Naeve CW, Pawlik CA, Houghton PJ, and Potter PM (1999) Comparison of activation of CPT-11 by rabbit and human carboxylesterases for use in enzyme/prodrug therapy. *Clin Cancer Res* **5:**917–924.

Dixon SL and Villar HO (1998) Bioactive diversity and screening library selection via affinity fingerprinting. *J Chem Inf Comput Sci* **38:**1192–1203.

Doctor BP, Toker L, Roth E, and Silman I (1987) Microtiter assay for acetylcholinesterase. *Anal Biochem* **166:**399–403.

Ellman GL, Courtney KD, Anders V, and Featherstone RM (1961) A new and rapid colorimetric determination of acetylcholinesterase activity. *Biochem Pharmacol* **7:**88–95.

Furman WL, Stewart CF, Poquette CA, Pratt CB, Santana VM, Zamboni WC, Bowman LC, Ma MK, Hoffer FA, Meyer WH, et al. (1999) Direct translation of a protracted irinotecan schedule from a xenograft model to a phase I trial in children. *J Clin Oncol* **17:**1815–1824.

Guichard S, Morton CL, Krull EJ, Stewart CF, Danks MK, and Potter PM (1998) Conversion of the CPT-11 metabolite APC to SN-38 by rabbit liver carboxylesterase. *Clin Cancer Res* **4:**3089–3094.

Houghton JA, Cheshire PJ, Hallman JA, Lutz L, Luo X, Li Y, and Houghton PJ (1996) Evaluation of irinotecan in combination with 5-fluorouracil or etoposide in xenograft models of colon adenocarcinoma and rhabdomyosarcoma. *Clin Cancer Res* **2:**107–118.

Houghton PJ, Cheshire PJ, Hallman JD 2nd, Lutz L, Friedman HS, Danks MK and Houghton JA (1995) Efficacy of topoisomerase I inhibitors, topotecan and irinotecan, administered at low dose levels in protracted schedules to mice bearing xenografts of human tumors. *Cancer Chemother Pharmacol* **36:**393–403.

Jakalian A, Jack DB, and Bayly CI (2002) Fast, efficient generation of high-quality atomic charges. AM1-BCC model: II. Parameterization and validation. *J Med Chem* **23:**1623–1641.

Kauvar LM, Higgins DL, Villar HO, Sportsman JR, Engqvist-Goldstein A, Bukar R, Bauer KE, Dilley H and Rocke DM (1995) Predicting ligand binding to proteins by affinity fingerprinting. *Chem Biol* **2:**107–118.

Khanna R, Morton CL, Danks MK, and Potter PM (2000) Proficient metabolism of CPT-11 by a human intestinal carboxylesterase. *Cancer Res* **60:**4725–4728.

Kiyama R, Tamura Y, Watanabe F, Tsuzuki H, Ohtani M, and Yodo M (1999) Homology modeling of gelatinase catalytic domains and docking simulations of novel sulfonamide inhibitors. *J Med Chem* **42:**1723–1738.

Kraulis PJ (1991) MOLSCRIPT: A program to produce both detailed and schematic plots of protein structures. *J Applied Crystallog* **24:**946–950.

MacPherson LJ, Bayburt EK, Capparelli MP, Carroll BJ, Goldstein R, Justice MR, Zhu L, Hu S, Melton RA, Fryer L, et al. (1997) Discovery of CGS 27023A, a non-peptidic, potent and orally active stromelysin inhibitor that blocks cartilage degradation in rabbits. *J Med Chem* **40:**2525–2532.

Merritt EA and Bacon DJ (1997) Raster 3D: Photorealistic molecular graphics. *Methods Enzymol* **277:**505–524.

Morton CL and Potter PM (2000) Comparison of *Escherichia coli, Saccharomyces cerevisiae*, *Pichia pastoris*, *Spodoptera frugiperda* and COS7 cells for recombinant gene expression: Application to a rabbit liver carboxylesterase. *Mol Biotechnol* **16:**193–202.

Morton CL, Taylor KR, Iacono L, Cheshire P, Houghton PJ, Danks MK, Stewart CF, and Potter PM (2002) Metabolism of CPT-11 in esterase deficient mice. *Proc Am Assoc Cancer Res* **43:**248.

Munger JS, Shi GP, Mark EA, Chin DT, Gerard C, and Chapman HA (1991) A serine esterase released by human alveolar macrophages is closely related to liver microsomal carboxylesterases. *J Biol Chem* **266:**18832–18838.

Potter PM and Danks MK (2000) Carboxylesterase-mediated activation of irinotecan. *Cancer Res Alert* **2:**80–83.

Potter PM, Pawlik CA, Morton CL, Naeve CW, and Danks MK (1998) Isolation and partial characterization of a cDNA encoding a rabbit liver carboxylesterase that activates the prodrug Irinotecan (CPT-11). *Cancer Res* **52:**2646–2651.

Satoh T, Hosokawa M, Atsumi R, Suzuki W, Hakusui H, and Nagai E (1994) Metabolic activation of CPT-11, 7-ethyl-10-[4-(1-piperidino)-1- piperidino]carbonyloxycamptothecin, a novel antitumor agent, by carboxylesterase. *Biol Pharm Bull* **17:**662–664.

Sawada S, Yokokura T, and Miyasaka T (1996) Synthesis of CPT-11 (irinotecan hydrochloride trihydrate). *Ann NY Acad Sci* **803:**13–28.

Schwer H, Langmann T, Daig R, Becker A, Aslanidis C, and Schmitz G (1997) Molecular cloning and characterization of a novel putative carboxylesterase, present in human intestine and liver. *Biochem Biophys Res Commun* **233:**117–120.

Tanizawa A, Fujimori A, Fujimori Y, and Pommier Y (1994) Comparison of topoisomerase I inhibition, DNA damage and cytotoxicity of camptothecin derivatives presently in clinical trials. *J Natl Cancer Inst* **86:**836–842.

Thompson J, Zamboni WC, Cheshire PJ, Lutz L, Luo X, Li Y, Houghton JA, Stewart CF, and Houghton PJ (1997a) Efficacy of systemic administration of irinotecan against neuroblastoma xenografts. *Clin Cancer Res* **3:**423–431.

Thompson J, Zamboni WC, Cheshire PJ, Richmond L, Luo X, Houghton JA, Stewart CF, and Houghton PJ (1997b) Efficacy of oral irinotecan against neuroblastoma xenografts. *Anticancer Drugs* **8:**313–322.

Tsuruo T, Matsuzaki T, Matsushita M, Saito H, and Yokokura T (1988) Antitumor effect of CPT-11, a new derivative of camptothecin, against pleiotropic drug-resistant tumors in vitro and in vivo. *Cancer Chemother Pharmacol* **21:**71–74.

Vedani A and Dobler M (2002a) 5D-QSAR: the key for simulating induced fit? *J Med Chem* **45:**2139–2149.

Vedani A and Dobler M (2002b) Multidimensional QSAR: Moving from three- to five-dimensional concepts. *Quant Struct-Act Relat* **21:**382–390.

Wadkins RM, Morton CL, Weeks JK, Oliver L, Wierdl M, Danks MK, and Potter PM (2001) Structural constraints affect the metabolism of 7-ethyl-10-[4-(1-piperidino)-1-piperidino]carbonyloxycamptothecin (CPT-11) by carboxylesterases. *Mol Pharmacol* **60:**355–362.

Webb JL (1963) *Enzyme and Metabolic Inhibitors. Volume 1. General Principles of Inhibition.* Academic Press Inc., New York, NY.

Whittaker M, Floyd CD, Brown P, and Gearing AJH (1999) Design and therapeutic applications of matrix metalloproteinase inhibitors. *Chem Rev* **99:**2735–2776.

Address correspondence to: Dr. Philip M. Potter, Department of Molecular Pharmacology, St. Jude Children's Research Hospital, 332 N. Lauderdale, Memphis, TN 38105. E-mail: phil.potter@stjude.org